Tokyo Climate Center, Japan Meteorological Agency

TCC News

No. 28 Spring 2012

Contents Page

El Niño Outlook (April – October 2012)

It is likely that neutral conditions will continue throughout the Northern Hemisphere summer.

El Niño/La Niña

In March 2012, the NINO.3 SST deviation was -0.2°C. SSTs in the equatorial Pacific were below normal mainly in the central part, while above-normal values were observed in the eastern part (Figures 1 and 3 (a)). Positive subsurface temperature anomalies were maintained in the western equatorial Pacific, while negative values in the eastern part almost disappeared (Figures 2 and 3 (b)). These oceanic characteristics indicate the persistence of ENSO-neutral conditions. In the atmosphere, convective activity was above normal over and around Indonesia. Over the western equatorial Pacific, easterly winds in the lower troposphere were stronger than normal in early March and weaker than normal in late March.

According to JMA's El Niño prediction model, the NINO.3 SST will be normal in the Northern Hemisphere spring and above normal in summer (Figure 4). Although the development of El Niño conditions in summer is possible, the uncertainty of the prediction is large for the summer and beyond. Considering the bias characteristics of the prediction, it is more likely that ENSO-neutral conditions will persist throughout the summer.

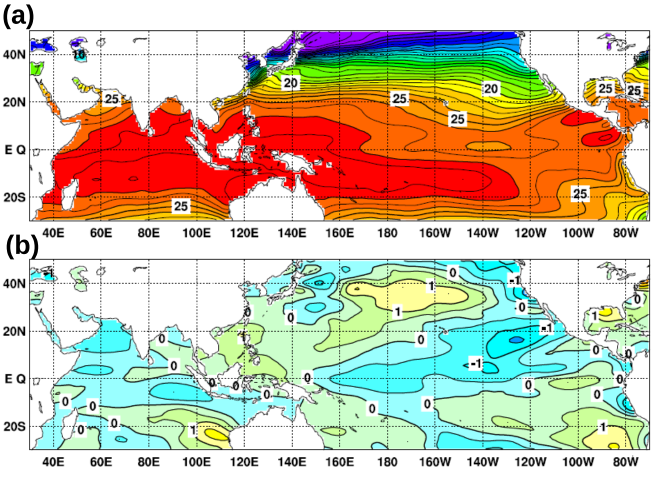

Figure 1 Monthly mean (a) sea surface temperatures (SSTs) and (b) SST anomalies in the Indian and Pacific Ocean areas for March 2012
Contour intervals are 1˚C in (a) and 0.5˚C in (b). The base period for the normal is 1981 – 2010.

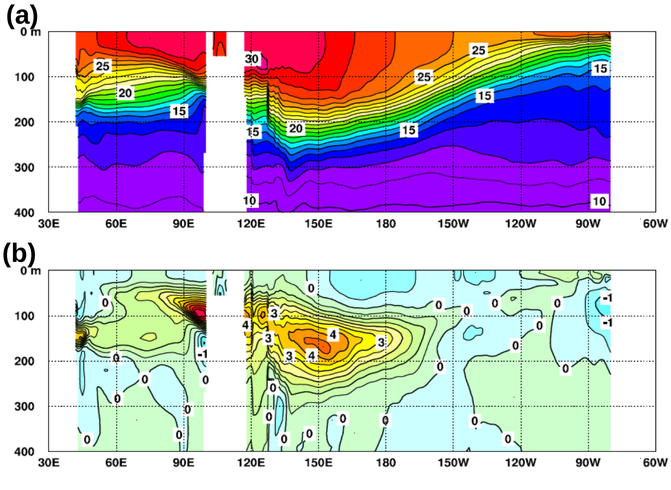

Figure 2 Monthly mean depth-longitude cross sections of (a) temperatures and (b) temperature anomalies in the equatorial Indian and Pacific Ocean areas for March 2012
Contour intervals are 1˚C in (a) and 0.5˚C in (b). The base period for the normal is 1981 – 2010.

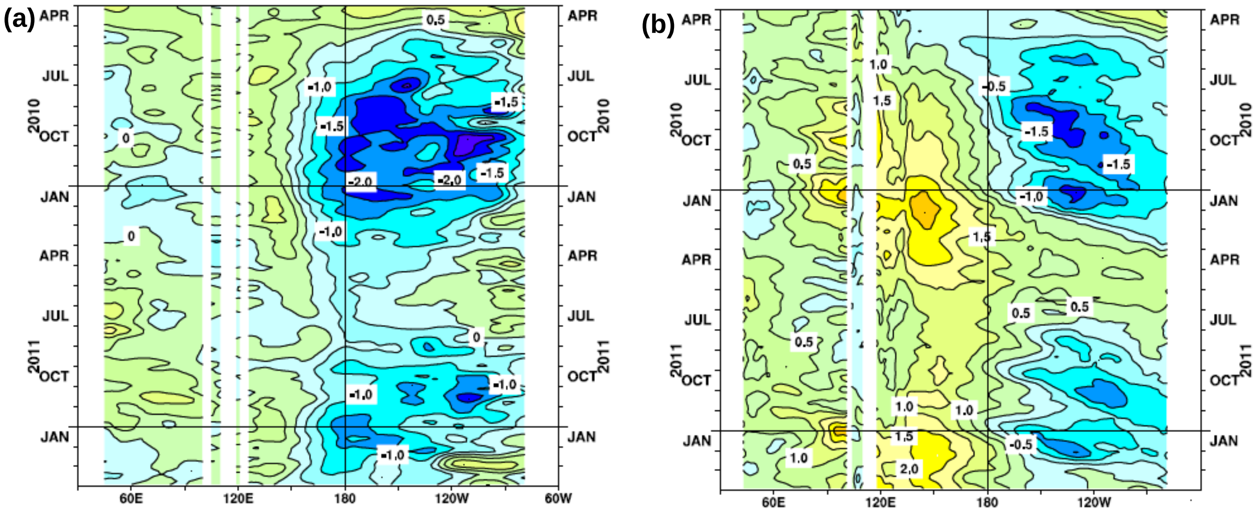

Figure 3 Time-longitude cross sections of (a) SST and (b) ocean heat content (OHC) anomalies along the equator in the Indian and Pacific Ocean areas
OHCs are defined here as vertical averaged temperatures in the top 300m. The base period for the normal is 1981 – 2010.

Western Pacific and Indian Ocean

The SST in the tropical western Pacific (NINO.WEST) region was near normal in March, and is likely to be near normal throughout the Northern Hemisphere summer.

The SST in the tropical Indian Ocean (IOBW) region was below normal in March. It is likely to gradually approach a normal level over the coming months, and will be near normal in the Northern Hemisphere summer.

(Ichiro Ishikawa, Climate Prediction Division)

* The SST normals for the NINO.WEST region (Eq. – 15°N, 130°E – 150°E) and the IOBW region (20°S – 20°N, 40°E – 100°E) are defined as linear extrapolations with respect to a sliding 30-year period in order to remove the effects of long-term trends.

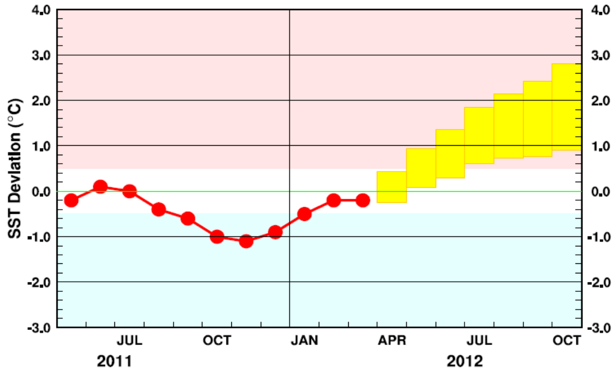

Figure 4 Outlook of the NINO.3 SST deviation produced by the El Niño prediction model
This figure shows a time series of the monthly NINO.3 SST deviations. The thick line with closed circles shows observed SST deviations, and the boxes show the values produced for the next six months by the El Niño prediction model. Each box denotes the range into which the SST deviation is expected to fall with a probability of 70%.

JMA's Seasonal Numerical Ensemble Prediction for Summer 2012

According to JMA's seasonal numerical prediction model, sea surface temperature (SST) anomalies in the eastern equatorial Pacific will be above normal this summer, suggesting a transition to El Niño-like conditions. In line with this prediction, active convection in the central equatorial Pacific and a southward shift of the sub-tropical jet are expected. However, as prediction skill in relation to El Niño/La Niña conditions from spring through summer is relatively low at the end of La Niña periods, it should be noted that the extent of atmospheric influence from the predicted El Niño-like SST anomalies is uncertain. Conversely, active convection to the east of the Philippines and inactive convection over the Maritime Continent and the northern part of the Indian Ocean are predicted.

1. Introduction

This article outlines JMA's dynamical seasonal ensemble prediction for summer (June – August) 2012, which was used as a basis for the Agency's operational warm-season outlook issued on 25 April 2012. This prediction is based on the seasonal ensemble prediction system used in conjunction with the Atmosphere-Ocean General Circulation Model (AOGCM). Please refer to the separate column for details of the system.

Section 2 outlines the global SST anomaly predictions, and Section 3 describes the circulation fields expected over the tropics and sub-tropics in association with these anomalies. Finally, the circulation fields predicted for the mid- and high latitudes of the Northern Hemisphere are explained in Section 4.

2. SST anomalies (Figure 5)

The predicted SST anomalies are shown in Figure 5. Above-normal values are expected in the eastern equatorial Pacific, suggesting a transition to El Niño-like conditions. However, hindcast experimentation indicates that JMA's model tends to predict a quicker transition to El Niño conditions and that the prediction skill for El Niño/La Niña conditions from spring through summer is relatively low at the end of La Niña periods. Accordingly, JMA's El Niño Outlook (http://ds.data.jma.go.jp/tcc/tcc/products/elnino/outlook.html) predicts that ENSO-neutral conditions are likely to continue during the summer. Meanwhile, above-normal SSTs are expected in the western tropical Pacific despite the predicted El Niño-like SST anomalies. In the tropical Indian Ocean, near-normal SSTs are predicted.

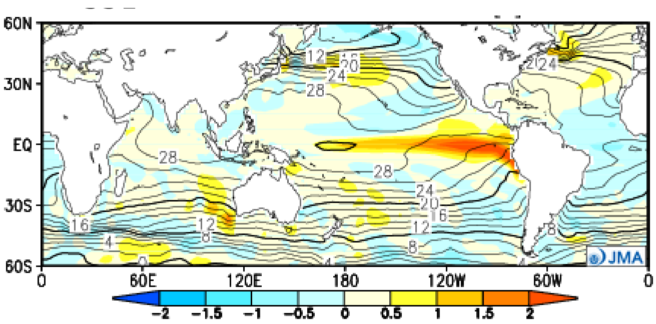

Figure 5 Predicted SSTs (contours) and SST anomalies (shading) for June – August 2012 (ensemble mean of 51 members)

3. Prediction for the tropics and sub-tropics (Figure 6)

Above-normal precipitation is predicted (a) from the central to the eastern equatorial Pacific and (b) to the east of the Philippines. Considering the uncertainty of the prediction for a transition to El Niño-like conditions, the above-normal precipitation prediction in (a) should be interpreted with caution. However, that in (b) can be reasonably expected in response to high SSTs over the western tropical Pacific. Below-normal precipitation is expected over the Maritime Continent and the northern part of the Indian Ocean.

In the upper troposphere, a negative-velocity (i.e., more divergent) potential anomaly at 200 hPa is predicted over the tropical Pacific, while positive (i.e., more convergent) anomalies are expected over the tropical Indian Ocean, reflecting the precipitation anomaly patterns in the tropics.

The stream function at 200 hPa is generally expected to be negative in the Northern Hemisphere, reflecting the zonal pattern of precipitation (i.e., active near the equator and inactive with increasing distance from it). This indicates a southward-shifting tendency for the sub-tropical jet. However, considering that these anomaly patterns may reflect the predicted El Niño-like SST anomalies, they should be interpreted with caution. Positive (i.e., anti-cyclonic) anomalies are expected to the east of the Philippines, reflecting above-normal precipitation in the region.

Stream function anomalies at 850 hPa are expected to be negative (i.e., cyclonic) to the east of the Philippines, suggesting development of the monsoon trough in the region. Meanwhile, positive (i.e., anti-cyclonic) anomalies are expected over the eastern part of the Indian Ocean, reflecting inactive convection in the region.

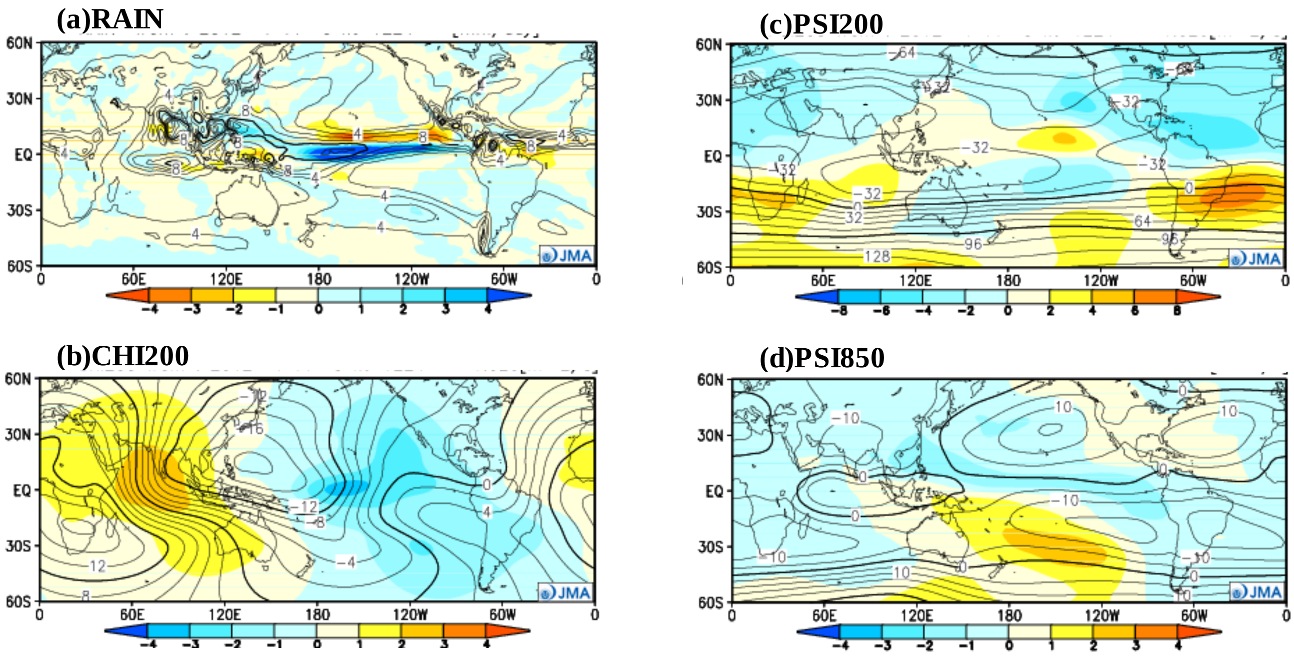

Figure 6 Predicted atmospheric fields from 60°N – 60°S for June – August 2012 (ensemble mean of 51 members)

(a) Precipitation (contours) and anomaly (shading). The contour interval is 2 mm/day.

(b) Velocity potential at 200 hPa (contours) and anomaly (shading). The contour interval is 2×10^6 m^2/s.

(c) Stream function at 200 hPa (contours) and anomaly (shading). The contour interval is 16×10^6 m^2/s.

(d) Stream function at 850 hPa (contours) and anomaly (shading). The contour interval is 5×10^6 m^2/s.

4. Prediction for the mid- and high latitudes of the Northern Hemisphere (Figure 7)

Negative anomalies of sea level pressure are predicted in most regions of the North Pacific High. However, positive anomalies are expected only in the western part in association with active convection to the east of the Philippines. Geo-potential height anomalies at 500 hPa are expected to be positive over almost the whole of the Northern Hemisphere, reflecting the influence of the recent warming trend.

(Masayuki Hirai, Climate Prediction Division)

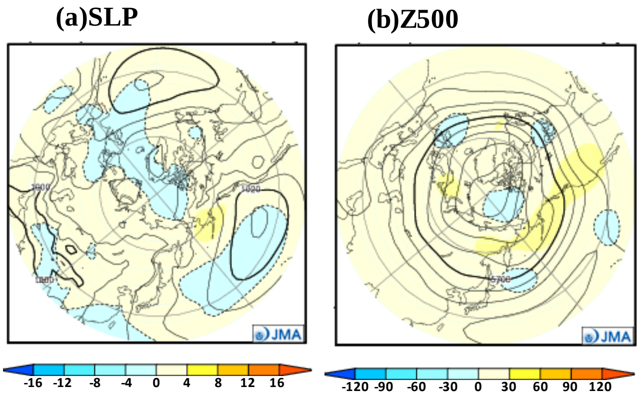

Figures 7 Predicted atmospheric fields from 20°N – 90°N for June – August 2012 (ensemble mean of 51 members)
(a) Sea level pressure (contours) and anomaly (shading). The contour interval is 4 hPa.
(b) 500 hPa height (contours) and anomaly (shading). The contour interval is 60 m.

JMA's Seasonal Ensemble Prediction System

JMA operates a seasonal Ensemble Prediction System (EPS) using the Atmosphere-Ocean General Circulation Model (AOGCM) to make seasonal predictions beyond a one-month time range. The EPS produces perturbed initial conditions by means of a combination of the initial perturbation method and the lagged average forecasting (LAF) method. The prediction is made using 51 members from the latest six initial dates (nine members are run every five days). Details of the prediction system and verification maps based on 30-year hindcast experiments (1979 – 2008) are available at http://ds.data.jma.go.jp/tcc/tcc/products/model/.

Warm Season Outlook for Summer 2012 in Japan

For summer 2012, mean temperatures are likely to be near normal or above normal, both with 40% probability, in western Japan and Okinawa/Amami. No particular characteristics are expected in terms of warm-season precipitation amounts in any region.

1. Outlook summary

JMA issued its outlook in relation to the area over Japan for the coming summer in February, and updated it in March and April. For summer 2012, mean temperatures are likely to be near normal or above normal, both with 40% probability, in western Japan and Okinawa/Amami. No particular characteristics are expected during the warm season or the rainy season (Baiu) in terms of precipitation amounts in any region (Figures 8 and 9).

2. Outlook background

JMA's coupled global circulation model predicts that SST anomalies averaged over the NINO.3 region will be above normal in summer 2012. However, the prediction accuracy of NINO.3's SST in summer is relatively low around the end of La Niña periods in spring. Accordingly, it is considered that SST anomalies in NINO.3 will be mostly near normal this summer. SSTs in the tropical Indian Ocean (IOBW) and in the western equatorial Pacific are both expected to be near normal in summer 2012.

Three-month precipitation anomalies are predicted to be above normal over central and eastern parts of the equatorial Pacific, and atmospheric circulation anomaly patterns over the tropical and sub-tropical Pacific are predicted to be similar to those seen during El Niño periods. Moreover, 850-hPa temperatures over northern Japan are predicted to be lower than those of the climatic normal. As such anomalous patterns are considered to appear due to predicted El Niño-like SST anomalies, the predictions should be treated with caution.

Conversely, as positive anomalies of three-month precipitation around the Philippines are predicted, it is con-

Category	−	0	+
Northern Japan	30	40	30
Eastern Japan	30	30	40
Western Japan	20	40	40
Okinawa and Amami	20	40	40

(Category −: below normal, 0 : normal, + : above normal, Unit : %)

Figure 8 Outlook for summer 2012 temperature probability in Japan

sidered that the extension of the North Pacific high will be almost normal around Japan during the summer in spite of the predicted El Niño-like SST anomalies. The Tibetan High is also expected to be normal. These results indicate that the circulation pattern around Japan will be almost normal in summer.

However, 500-hPa height anomalies are predicted to be positive over almost the whole of the Northern Hemisphere due to the influence of the recent warm trend. Furthermore, a tendency for above-normal temperatures has been observed in all regions over the last 10 years, indicating that this summer-averaged temperature tends to be above normal in Japan.

In terms of atmospheric circulation around Japan, the intensities of the North Pacific High and the Tibetan High are expected to be almost normal. However, due to the influence of the recent warm trend, temperatures are expected to be above normal nationwide. As for temperatures in northern and eastern Japan, the probability of above-normal values is reduced to a certain extent in consideration of the possibility of El Niño-like SST patterns.

(Takafumi Umeda, Climate Prediction Division)

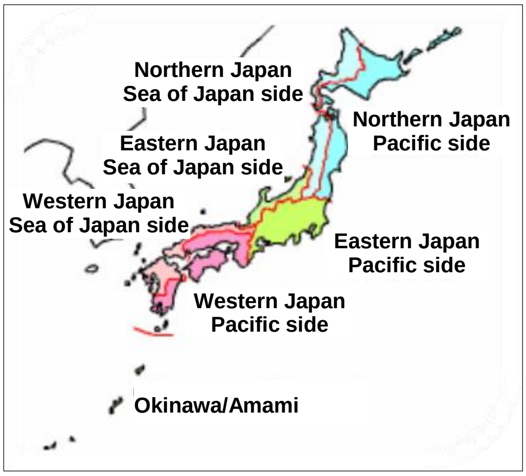

Category		−	0	+
Northern Japan	Sea of Japan side	30	40	30
	Pacific side	30	40	30
Eastern Japan	Sea of Japan side	30	40	30
	Pacific side	30	40	30
Western Japan	Sea of Japan side	30	40	30
	Pacific side	30	40	30
Okinawa and Amami		30	40	30

(Category −: below normal, 0 : normal, + : above normal, Unit : %)

Figure 9 Outlook for summer 2012 precipitation probability in Japan

Asian Winter Monsoon Summary for 2011/2012

Many parts of East and Central Asia experienced significantly below-normal temperatures throughout winter (December – February) 2011/2012. This report summarizes the related surface climate characteristics, atmospheric circulation and primary factors contributing to the cold conditions observed. The relevant factors were clarified based on investigation by JMA's Advisory Panel on Extreme Climate Events. (For details of the panel, see the related article on page 12.)

Note: JRA/JCDAS (Onogi et al. 2007) atmospheric circulation data and COBE-SST (JMA 2006) sea surface temperature (SST)/sea ice concentration data were used for this investigation. The outgoing longwave radiation (OLR) data referenced to infer tropical convective activity were originally provided by NOAA. The base period for the normal is 1981 – 2010.

1. Surface climate conditions

In winter 2011/2012, Asian countries in the mid-latitudes experienced significantly lower-than-normal temperatures due to strong cold-air inflow, while the northern part of Siberia and southern Asian countries experienced higher-than-normal temperatures (Figure 10). Figure 11 shows extreme climate events that occurred from December 2011 to February 2012. In December 2011, extremely low temperatures were observed in eastern Mongolia and southern Central Asia, while extremely high temperatures were seen from northern Central Siberia to northern Western Siberia. In January, extremely low temperatures were observed around Mongolia, and extremely light precipitation amounts (snow) were seen from the southern part of Western Siberia to Kazakhstan. In February, extremely low temperatures were observed from central Mongolia to the Middle East, while extremely high temperatures were seen from northern Central Siberia to northern Western Siberia. Extremely light precipitation (snow) amounts were observed from Western Siberia to northern Kazakhstan.

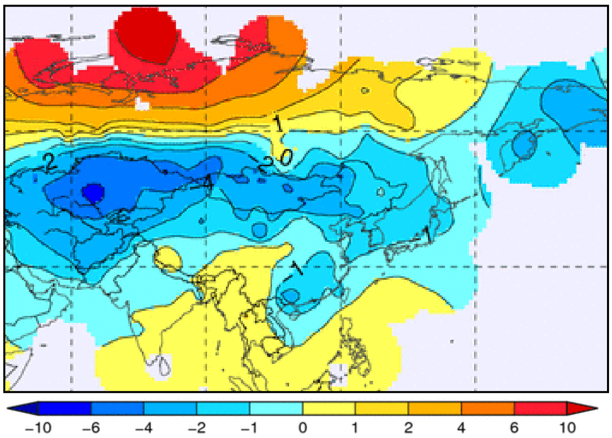

Figure 10 Seasonal temperature anomalies for winter (December – February) 2011/2012

Anomalies are deviations from the normal (i.e., the 1981 – 2010 average). The contour interval is 1°C.

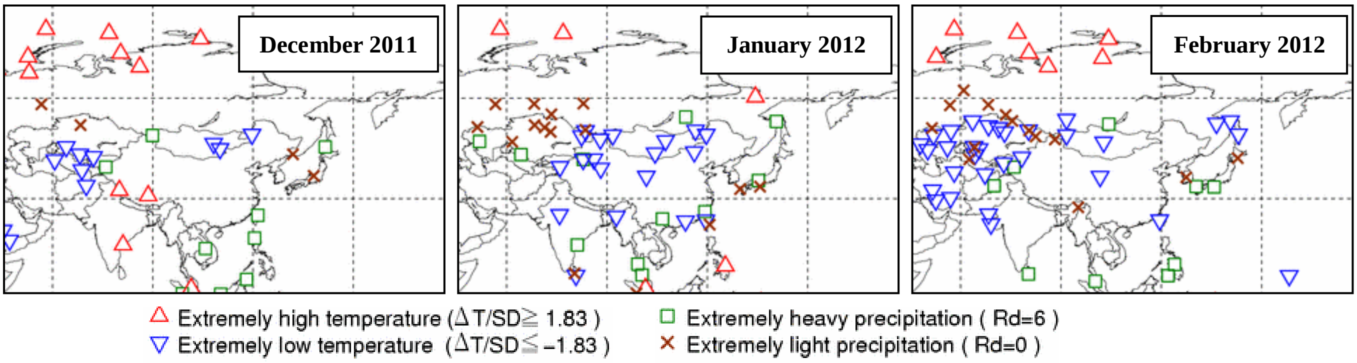

Figure 11 Extreme climate events from December 2011 to February 2012

2. Characteristic atmospheric circulation causing the cold winter conditions

In the 500-hPa height field for boreal winter 2011/2012 (Figure 12 (a)), distinct wave trains were observed from the North Atlantic to Eurasia with positive anomalies over western Siberia and negative anomalies over northeastern Asia, indicating significant meandering of the polar front jet stream. This wavy pattern persisted throughout the winter (Figure 13), forming in association with stationary Rossby wave packets propagating eastward from the North Atlantic (Figure 14).

In the sea level pressure field (Figure 12 (b)), positive anomalies were seen across northern Eurasia, and especially over western Siberia. The Siberian High was significantly enhanced and expanded, reaching its strongest level since 1979/1980 (Figure 15). The intensification of the Siberian High was associated with upper-level ridges over western Siberia (Takaya and Nakamura 2005a and 2005b) (Figure 16). The enhanced Siberian High contributed to an intensification of the East Asian winter monsoon, which strengthened cold air advection over the region.

In the 850-hPa temperature field (Figure 12 (c)), negative anomalies were seen in the mid-latitudes of Eurasia, especially over Central and East Asia. In the lower troposphere, anticyclonic circulation anomalies centered over western Siberia brought a cold air mass from central and eastern Siberia to Central Asia and Mongolia, contributing to extremely below-normal temperatures in the latter areas and enhancing the Siberian High (Figure 17). Anticyclonic circulation anomalies over western Siberia were associated with the upper-level blocking ridges there.

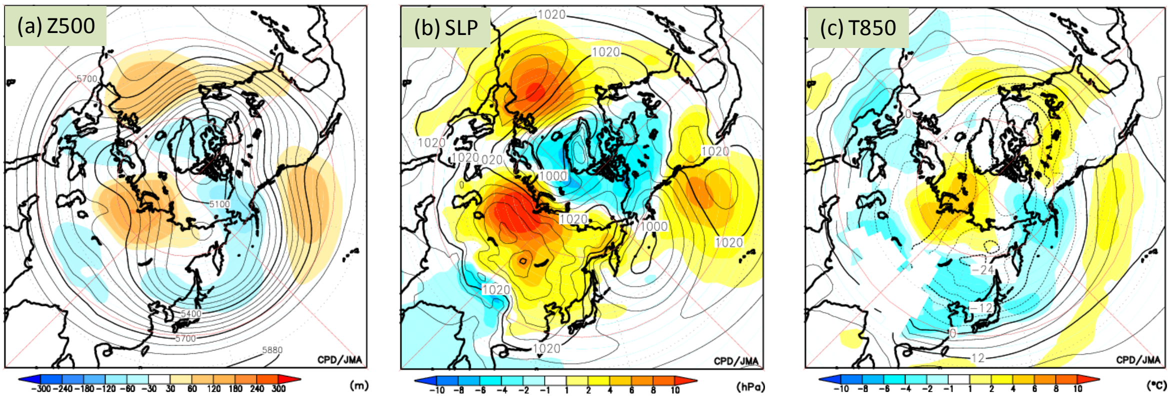

Figure 12 Three-month mean (a) 500-hPa height, (b) sea level pressure and (c) 850-hPa temperature for December 2011 – February 2012

The contour intervals are (a) 60 m, (b) 4 hPa and (c) 4˚C. The shading indicates respective anomalies (i.e., deviations from the 1981 – 2010 average). Contours/shading are not shown for areas with altitudes exceeding 1,600 m.

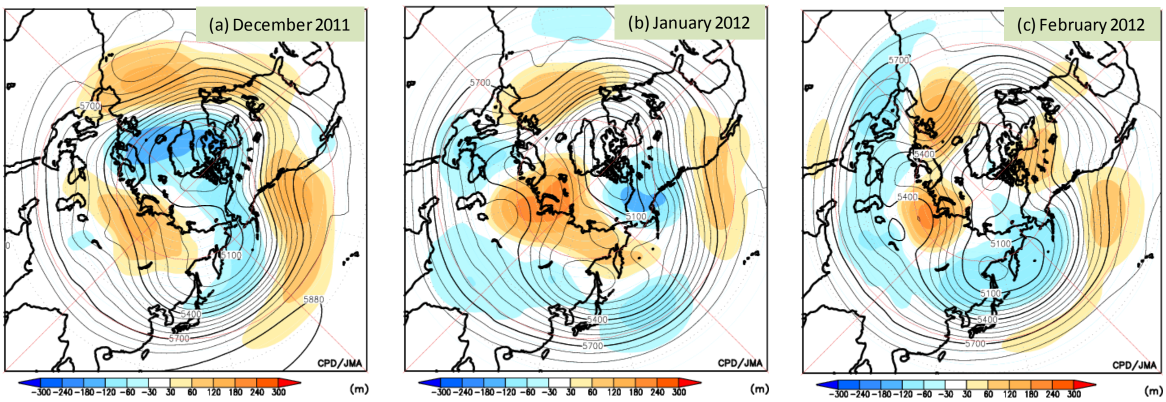

Figure 13 Monthly mean 500-hPa height for (a) December 2011, (b) January 2012 and (c) February 2012

The contour intervals are 60 m, and the shading indicates 500-hPa height anomalies.

In the upper troposphere, Rossby wave packets propagated eastward from southern China to the area east of Japan (Figure 14). Distinct anticyclonic circulation anomalies were seen over the former area and cyclonic circulation anomalies were observed over the latter. In line with these conditions, northerly wind anomalies were seen over Japan, indicating a southward meandering of the subtropical jet stream around the country (Figure 18). In association, upper-level cold air frequently moved into Japan, contributing to below-normal temperatures over the country and heavy snowfall on its Sea of Japan side.

In the zonally averaged fields over the mid-latitudes from central to eastern Eurasia, temperatures were below normal throughout the whole of the troposphere, and geopotential heights were below and above normal in the upper and lower troposphere, respectively (Figure 19).

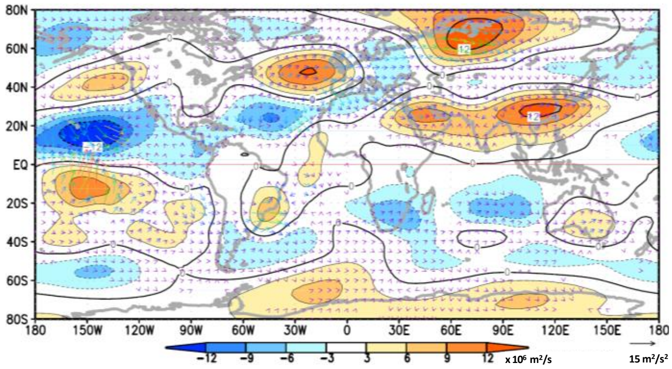

Figure 14 Three-month mean 200-hPa stream function anomalies and wave activity flux for December 2011 – February 2012

The contours and shading indicate stream function anomalies at intervals of 3 × 10^6 m^2/s. The warm- (cold)-color shading denotes anticyclonic (cyclonic) circulation anomalies in the Northern Hemisphere, and vice versa in the Southern Hemisphere. The vectors show wave activity flux (unit: m^2/s^2) based on Takaya and Nakamura (2001).

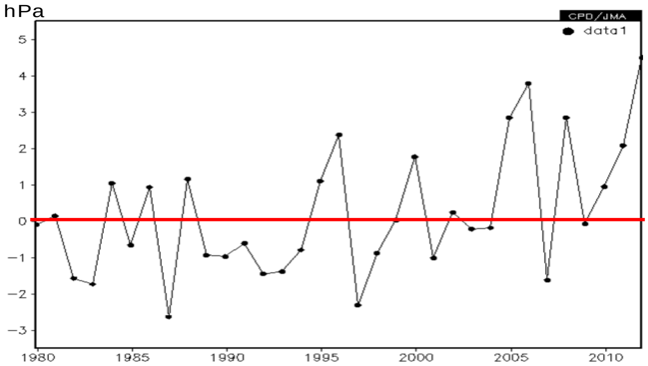

Figure 15 Interannual variation of area-averaged sea level pressure anomalies (unit: hPa) around the center of the Siberian High (40˚N – 60˚N, 80˚E – 120˚E) for winters (December – February) from 1979/1980 to 2011/2012

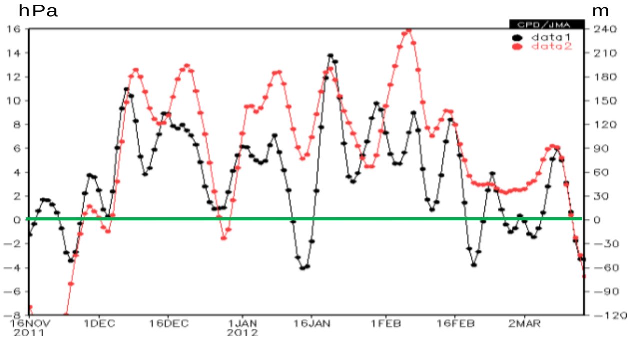

Figure 16 Time series of area-averaged sea level pressure anomalies around the center of the Siberian High (40˚N – 60˚N, 80˚E – 120˚E) and area-averaged 500-hPa height anomalies over western Siberia (50˚N – 70˚N, 60˚E – 90˚E) from 16 November 2011 to 15 March 2012

The black and red lines indicate five-day running mean values of area-averaged sea level pressure anomalies (unit: hPa) and 500-hPa height anomalies (unit: m), respectively. The coefficient of correlation between them for the period from 1 December, 2011, to 29 February, 2012, is 0.60 (with a 95% confidence level).

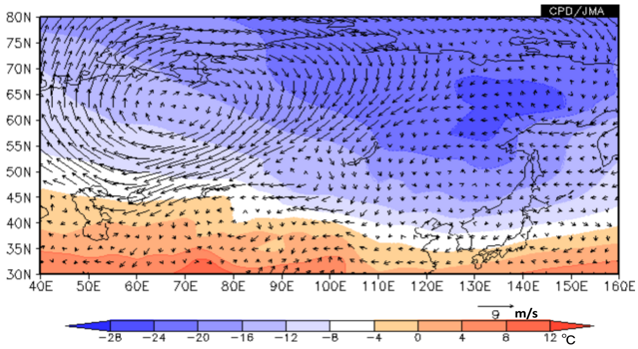

Figure 17 Three-month mean 850-hPa wind vector anomalies and 850-hPa normal temperatures for December 2011 – February 2012

The vectors indicate wind vector anomalies (unit: m/s), and the shading denotes normal temperatures (unit: ˚C; 1981 – 2010 average).

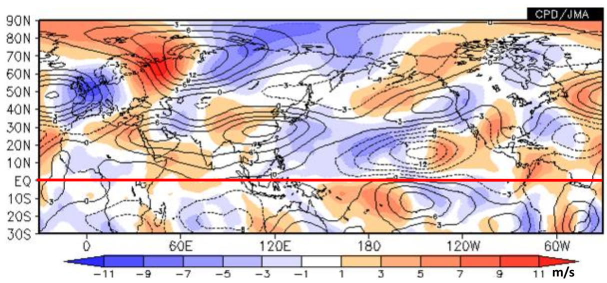

Figure 18 Three-month mean 200-hPa stream function anomalies and meridional wind anomalies for December 2011 – February 2012

The contours denote stream function anomalies at intervals of 3 × 10^6 m^2/s. The shading indicates meridional wind anomalies (unit: m/s), and positive (warm-color) and negative (cold-color) values denote southerly (northerly) wind anomalies, respectively.

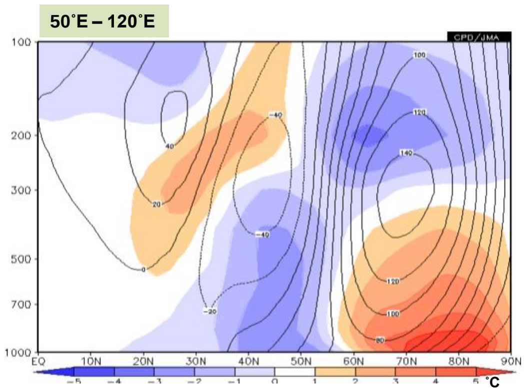

Figure 19 Latitude-height cross section of three-month mean geopotential height anomalies and temperature anomalies zonally averaged between 50˚E – 120˚E for December 2011 – February 2012

The contours denote geopotential height anomalies at intervals of 20 m. The shading indicates temperature anomalies (unit: ˚C).

3. Primary factors

3.1 Southward meandering of the subtropical jet stream around Japan

In winter 2011/2012, SST anomaly patterns in the Pacific exhibited La Niña-like conditions* (Figure 20 (a)), and convective activity was enhanced around the Maritime Continent throughout the season (Figure 20 (b)). It can be inferred that this active convection led to the upper-level anticyclonic circulation anomalies seen around southern China by forcing a Gill-type response (Gill 1980) (Figure 20 (b)). These anomaly patterns in convective activity and atmospheric circulation are typical of past La Niña events (Figure 21). Accordingly, the southward meandering of the subtropical jet stream around Japan, which caused frequent cold air flows over the country, was considered to be associated with the La Niña-like conditions.

* JMA defines a La Niña event as a phenomenon in which the five-month running-mean values of monthly SST deviations from the sliding 30-year mean for the El Niño monitoring region (NINO.3: 5˚S – 5˚N, 150˚W – 90˚W) stay at -0.5˚C or below for six consecutive months or longer. As SST values remained below -0.5˚C for only five consecutive months from September 2011 to January 2012, the criteria for JMA's La Niña definition were not met.

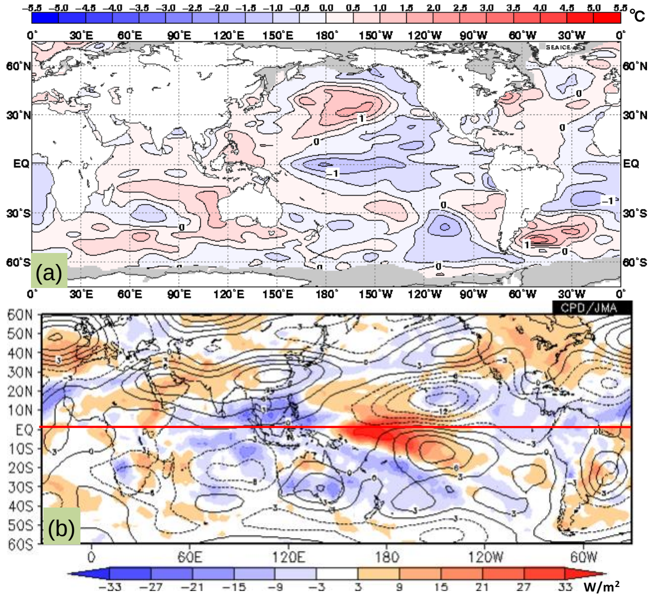

Figure 20 Three-month mean (a) sea surface temperature (SST) anomalies and (b) 200-hPa stream function anomalies and outgoing longwave radiation (OLR) anomalies for December 2011 – February 2012

(a) The contours and shading indicate SST anomalies at intervals of 0.5˚C. (b) The contours denote stream function anomalies at intervals of 3 × 10^6 m^2/s, and the shading indicates OLR anomalies (unit: W/m^2). The cold- (warm-) color shading denotes enhanced (suppressed) convective activity.

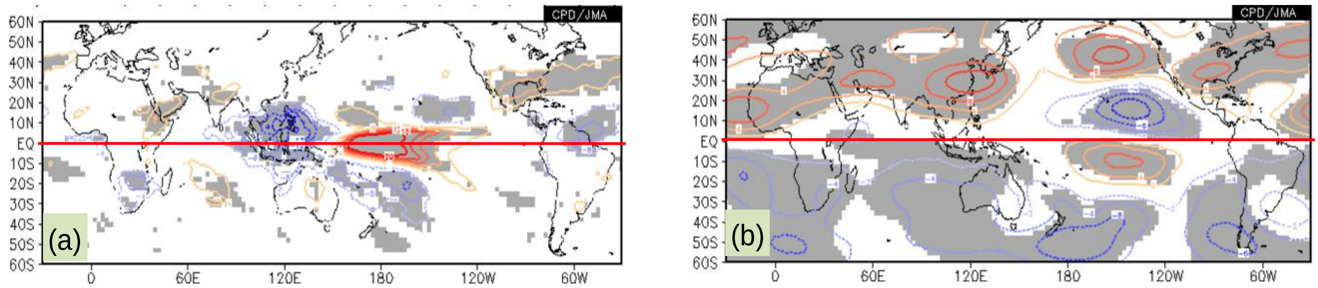

Figure 21 La Niña composites of three-month mean (a) outgoing longwave radiation (OLR) anomalies and (b) 200-hPa stream function anomalies for December – February

(a) The contours indicate OLR anomalies at intervals of 4 W/m^2 (shown between -20 W/m^2 and 20 W/m^2). (b) The contours denote stream function anomalies at intervals of 3 × 10^6 m^2/s. (a) and (b) The past La Niña winters (December – February) selected for the composites are those of 1984/1985, 1988/1989, 1995/1996, 1998/1999, 1999/2000, 2005/2006 and 2007/2008. The gray shading indicates a 95% confidence level as indicated by t-testing.

3.2 Significant meandering of the polar front jet stream over Eurasia

The wave trains along the polar jet stream over Eurasia that contributed to the intensification and northwestward expansion of the Siberian High mainly originated in the North Atlantic, where upper-level cyclonic and anticyclonic circulation anomalies were seen over subtropical and mid-latitude areas, respectively (Figure 14).

In past La Niña events (Figure 21), anticyclonic circulation anomalies tended to appear across the middle latitudes from the eastern North Pacific to the North Atlantic with three centers west of the USA, over southeastern parts of the country, and west of Europe. Related circulation anomalies for winter 2011/2012 (Figure 14) showed anomaly patterns typical of past events. Thus, La Niña-like conditions may be associated with the anticyclonic circulation anomalies observed in the North Atlantic mid-latitudes.

Significant divergence anomalies in the upper troposphere were seen around northern South America and the tropical North Atlantic in association with the enhanced convective activity observed there (Figure 22). Anomalous northward-flowing divergent winds seen on the northern side of the divergence converged over areas east of the Caribbean Sea where the Rossby wave source (Sardeshmukh and Hoskins 1988) exhibited positive values (indicating vorticity sources) (Figure 23). Active convection around northern South America and the tropical North Atlantic was therefore considered responsible for the generation of upper-level cyclonic circulation anomalies as an origin of the wave trains seen over the subtropical North Atlantic.

Active convection around northern South America and the tropical North Atlantic was also seen in past La Niña events (Figure 21 (a)). SSTs were above normal in northwestern parts of the tropical North Atlantic and significantly below normal in the tropical South Atlantic (Figure 20). Statistical analysis shows that convective activity over tropical areas tends to be enhanced when tropical SSTs are below normal in the tropical South Atlantic (Figure 24) and when dipole SST anomaly patterns with positive north and negative south values are seen in the tropical Atlantic (Figure 25).

Accordingly, it can be inferred that the SST anomalies observed in the tropical Atlantic and the La Niña-like conditions seen contributed to anomalous atmospheric circulation over the North Atlantic, thereby inducing eastward-stretching wave trains.

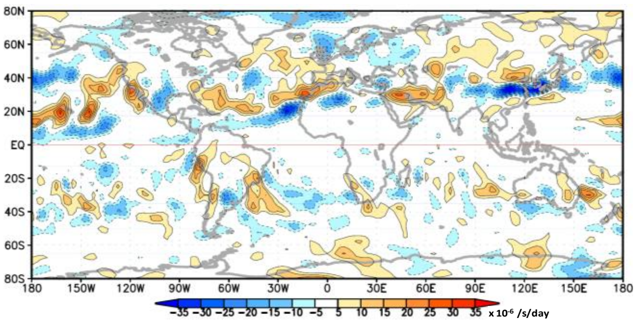

Figure 23 Rossby wave source anomalies at 200 hPa for December 2011 – February 2012

The contours and shading indicate Rossby wave source anomalies (unit: 5 × 10^{-6} /s/day). Positive (warm-color) and negative (cold-color) anomalies represent vorticity sources and sinks, respectively.

3.3 Low temperatures across the Eurasian mid-latitudes

In past La Niña periods, a tendency has been observed in the Eurasian mid-latitudes whereby temperatures in the troposphere and geopotential heights in the upper troposphere are lower than normal (without a 90% confidence level) (Figure 26). The related anomalies for winter 2011/2012 (Figures 12 and 19) echo this tendency. Steady response to diabatic heating anomalies around the Maritime Continent was examined using a linear baroclinic model (LBM; Watanabe and Kimoto 2000). The LBM results (Figure 27) indicated that both lower-level temperatures and upper-level height were below normal in the mid-latitudes of Eurasia, which was consistent with characteristics seen in past La Niña events.

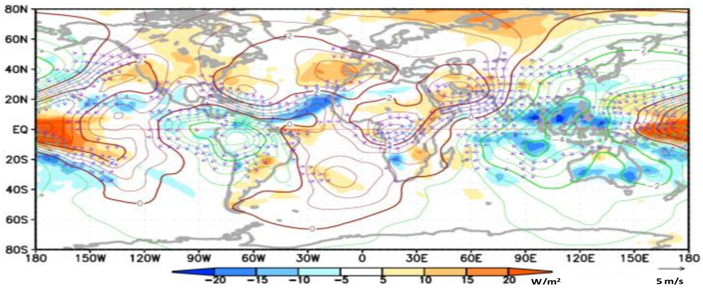

Figure 22 Three-month mean 200-hPa velocity potential anomalies, 200-hPa divergent wind anomalies and outgoing longwave radiation (OLR) anomalies for December 2011 – February 2012

The contours indicate velocity potential anomalies at intervals of 0.5 × 10^6 m^2/s. The vectors denote divergent wind anomalies (unit: m/s). The shading indicates OLR anomalies (unit: W/m^2). The cold- (warm-) color shading denotes enhanced (suppressed) convective activity.

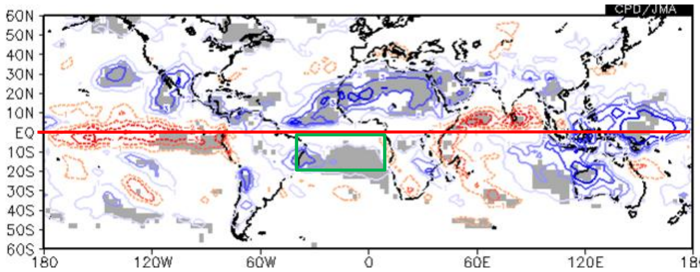

Figure 24 Three-month mean outgoing longwave radiation regressed onto area-averaged sea surface temperatures (unit: ˚C) in the tropical South Atlantic (green rectangle: 20˚S – eq., 40˚W – 10˚E) for winters (December – February) from 1979/1980 to 2010/2011

The contour intervals are 1 W/m^2, and positive and negative values are colored in blue and red, respectively. The gray shading indicates a 95% confidence level as indicated by t-testing.

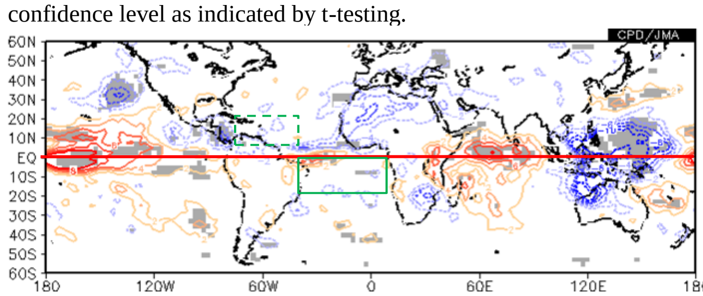

Figure 25 Composite of three-month mean outgoing longwave radiation anomalies for winter (December – February) when tropical sea surface temperatures were positive in the northwestern North Atlantic (dashed green rectangle: 5˚N – 20˚N, 75˚W – 40˚W) and negative in the South Atlantic (solid green rectangle: 20˚S – eq., 40˚W – 10˚E)

The winters selected for the composite are 1979/1980, 1980/1981, 1995/1996, 1996/1997, 2001/2002 and 2005/2006. The contour intervals are 2 W/m^2. The gray shading indicates a 95% confidence level as indicated by t-testing.

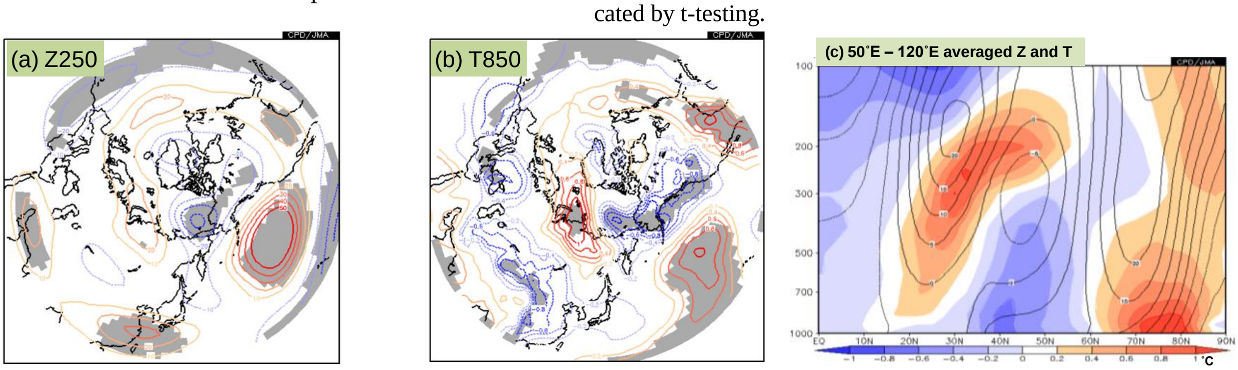

Figure 26 La Niña composites of three-month mean (a) 250-hPa height anomalies, (b) 850-hPa temperature anomalies, and (c) zonally-averaged geopotential height and temperature anomalies (50˚E – 120˚E) for winter (December – February)

(a) The contours indicate height anomalies at intervals of 10 m (shown between -50 m and 50 m). (b) The contours denote temperature anomalies at intervals of 0.2˚C (shown between -1˚C and 1˚C). (c) The contours denote geopotential height anomalies at intervals of 5 m, and the shading indicates temperature anomalies (unit: ˚C). (a) – (c) The past La Niña winters selected for the composites are those of 1984/1985, 1988/1989, 1995/1996, 1998/1999, 1999/2000, 2005/2006 and 2007/2008. The gray shading indicates a 90% confidence level as indicated by t-testing.

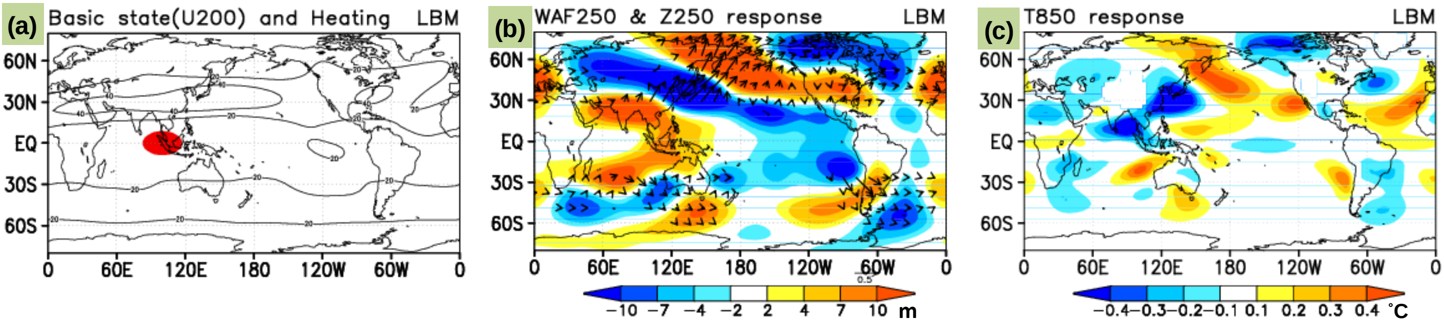

Figure 27 Steady response in a linear baroclinic model (LBM) to heating anomalies near the Maritime Continent
(a) The red ellipse indicates diabatic heating for the LBM with the basic state for January (i.e., the 1979 – 2004 average based on JRA-25 data). (b) The shading denotes the steady response of 250-hPa height anomalies (unit: m), and the vectors indicate wave activity fluxes (unit: m^2/s^2). (c) The shading indicates the steady response of 850-hPa temperature anomalies (unit: ˚C). (b) and (c) These anomalies as responses represent deviations from the respective basic states and are additionally subtracted from the zonal averages of the respective anomalies. The related steady responses to heating in the basic state for December and February (not shown) are similar to those for January.

Accordingly, the La Niña-like conditions observed may be responsible for low temperatures in the Eurasian middle latitudes.

3.4 Arctic sea ice

During winter 2011/2012, the sea ice extent in the Arctic Ocean, especially in the Barents Sea and the Kara Sea, remained far below the 1979 – 2000 average (Figure 28). According to statistical analysis (Figure 29), atmospheric circulation anomalies over Eurasia seen in light sea ice around the seas echoed related anomalies observed during the winter (Figure 12). Recent studies (e.g., Honda et al. 2009, Inoue et al. 2012) have reported that a reduction in the amount of floating sea ice tends to induce amplification of the Siberian High, leading to cold anomalies in East Asia. Thus, the light sea ice observed around the Barents Sea and the Kara Sea may contribute to the enhancement of the Siberian High.

4. Summary

In the 2011/2012 Asian winter monsoon season, Central and East Asia experienced cold winter conditions due to a strong Siberian High and frequent cold surges. The possible primary factors contributing to these conditions are summarized in Figure 30, but the related mechanisms have not yet been fully clarified.

(1: Kazuyoshi Yoshimatsu, 2-4: Shotaro Tanaka, Climate Prediction Division)

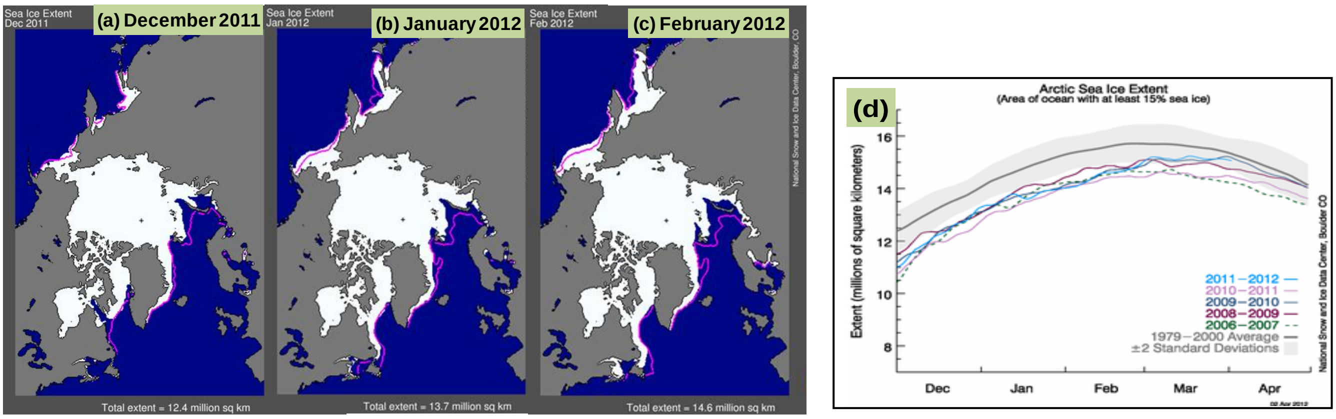

Figure 28 Arctic sea ice extent for winter 2011/2012
(a) – (c) Monthly Arctic sea ice extent for (a) December 2011, (b) January 2012 and (c) February 2012. The magenta line shows the 1979 to 2000 median extent for that month. The black cross marks the geographic North Pole. (d) Daily Arctic sea ice extent as of April 2, 2012, along with the corresponding values for the previous four years. The current year is shown in light blue, 2010 – 2011 in pink, 2009 – 2010 in dark blue, 2008 – 2009 in purple, and 2006 – 2007 (the year in which the record minimum was seen) in dashed green. The gray area around the average line shows the two-standard-deviation range of the data.
(Sources: National Snow and Ice Data Center (NSIDC), USA, at http://nsidc.org/arcticseaicenews/)

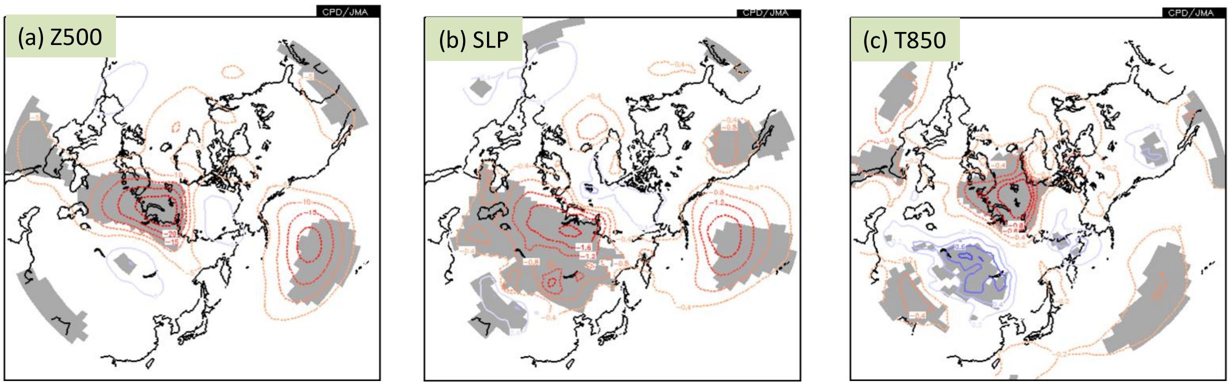

Figure 29 Three-month mean (a) 500-hPa height, (b) sea level pressure and (c) 850-hPa temperature regressed onto area-averaged sea ice extents around the Barents Sea and the Kara Sea (70˚N – 80˚N, 45˚E – 90˚E) for winters (December – February) from 1979/1980 to 2010/2011

The contour intervals are (a) 5 m, (b) 0.4 hPa, and (c) 0.2˚C. Warm- (cold-) color contours indicate negative (positive) values. The gray shading indicates a 90% confidence level as indicated by t-testing. COBE-SST sea ice concentration data were used for this analysis.

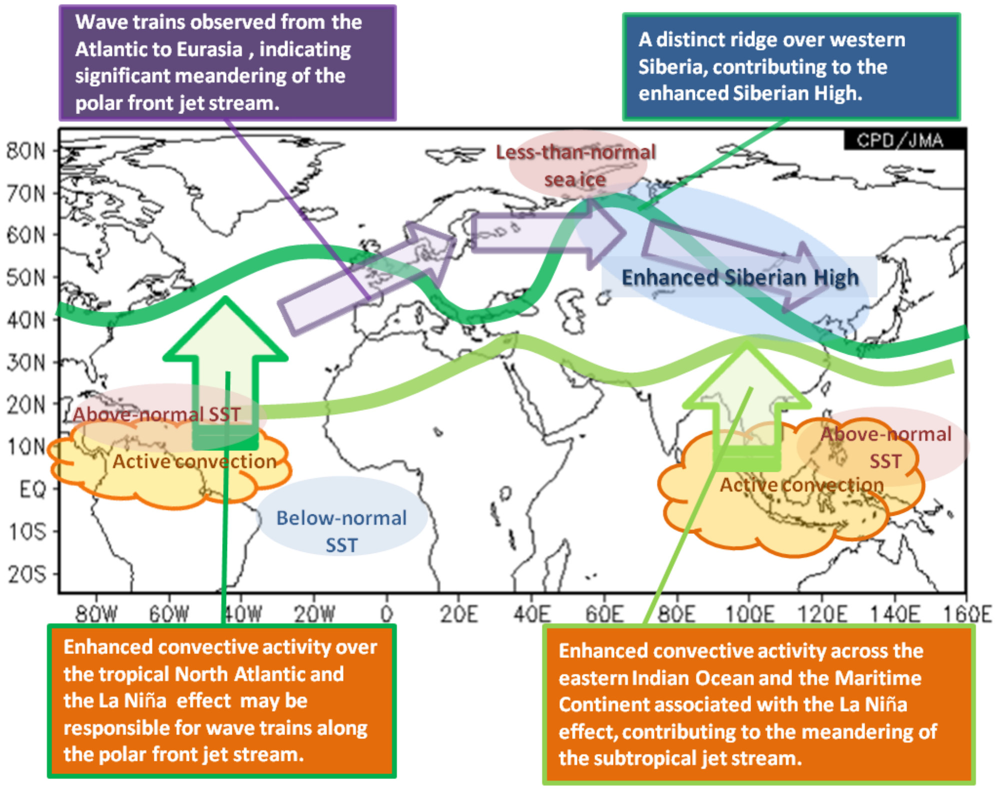

Figure 30 Primary factors contributing to cold winter conditions of 2011/2012 in Central and East Asia

References

Gill, A. E., 1980: Some simple solutions for heat-induced tropical circulation. *Quart. J. Roy. Meteor. Soc.*, **106**, 447 – 462.

Honda, M., J. Inoue, and S. Yamane, 2009: Influence of low Arctic sea-ice minima on anomalously cold Eurasian winters. *Geophys. Res. Lett.*, **36**, L08707, doi: 10.1029/2008GL037079.

Inoue, J., M. Hori, and K. Takaya, 2012: The Role of Barents Sea Ice in the Wintertime Cyclone Track and Emergence of a Warm-Arctic Cold-Siberian Anomaly. *J. Climate*, **25**, 2561 – 2568.

JMA, 2006: Characteristics of Global Sea Surface Temperature Data (COBE-SST), *Monthly Report on Climate System*, Separated Volume No. **12**.

Onogi, K., J. Tsutsui, H. Koide, M. Sakamoto, S. Kobayashi, H. Hatsushika, T. Matsumoto, N. Yamazaki, H. Kamahori, K. Takahashi, S. Kadokura, K. Wada, K. Kato, R. Oyama, T. Ose, N. Mannoji and R. Taira, 2007: The JRA-25 Reanalysis. *J. Meteorol. Soc. Japan*, **85**, 369 – 432.

Sardeshmukh, P. D., and B. J. Hoskins, 1988: The generation of global rotational flow by steady idealized tropical divergence. *J. Atmos. Sci.*, **45**, 1228 – 1251.

Takaya, K., and H. Nakamura, 2001: A formulation of a phase-independent wave-activity flux for stationary and migratory quasigeostrophic eddies on a zonally varying basic flow. *J. Atom. Sci.*, **58**, 608 – 627.

—, and —, 2005a: Mechanisms of intraseasonal amplification of the cold Siberian high. *J. Atmos. Sci.*, **62**, 4423 – 4440.

—, and —, 2005b: Geographical dependence of upper-level blocking formation associated with intraseasonal amplification of the Siberian high. *J. Atmos. Sci.*, **62**, 4441 – 4449.

Watanabe, M., and M. Kimoto, 2000: Atmospheric-ocean thermal coupling in North Atlantic: Apositive feedback, *Quart. J. R. Met. Soc.*, **126**, 3343 – 3369.

JMA's Advisory Panel on Extreme Climate Events

To support the provision of timely statements on primary factors relating to ongoing extreme climate events, the Japan Meteorological Agency (JMA) established the Advisory Panel on Extreme Climate Events in June 2007.

The Advisory Panel on Extreme Climate Events is tasked with investigating extreme climate events based on a climatological approach so that it can advise JMA in issuing statements on such events and recommend related application of the latest findings. The Panel consists of prominent climate scientists from Japanese universities and research institutes, and is chaired by Prof. Kimoto from the University of Tokyo.

Essentially, when a nationwide-scale extreme climate event that significantly impacts socio-economic activity occurs, the Panel initiates investigation and discussion of related factors with JMA experts. Following preliminary discussions, it holds a meeting at JMA's headquarters or online, after which JMA issues a statement on matters such as the outlook for the event based on the Panel's investigation and advice. The statement is provided to the general public and to decision makers in socio-economic sectors to help them avoid or minimize adverse effects from the event. Since the Panel was established in 2007, JMA has issued a number of statements, including those related to heat waves in summer 2008, the record-breaking hot summer of 2010 and the cold winter of 2011/2012.

JMA routinely shares information on the current conditions of the climate system and discusses climatic anomalies with the Panel using a dedicated website and e-mail communication. The Agency developed the Interactive Tools for Analysis of the Climate System (ITACS) for the Panel to support analysis of the causes of extreme climate events. ITACS is also provided to National Meteorological and Hydrological Services (NMHSs) to assist with their related activities.

The Panel also advises JMA in regard to the improvement of climate diagnosis tools. New approaches introduced by the Agency based on Panel advisories include a linearized baroclinic model (LBM) for the investigation of stationary response to convective heating anomalies and a method for diagnosing meridional-mean circulation using mass-weighted isentropic zonal mean (MIM) meridional velocity values.

Figure 31 shows the framework of the Panel, which is positioned between JMA and the climate research community. It can be seen that the framework supports favorable collaboration and cooperation between the academic and operational services sectors. Panel-related activities, including discussions on diagnostic analysis and sharing of the latest climatological findings, have helped JMA to enhance its ability for monitoring and analysis and to improve its climate services.

(Shotaro Tanaka, Climate Prediction Division)

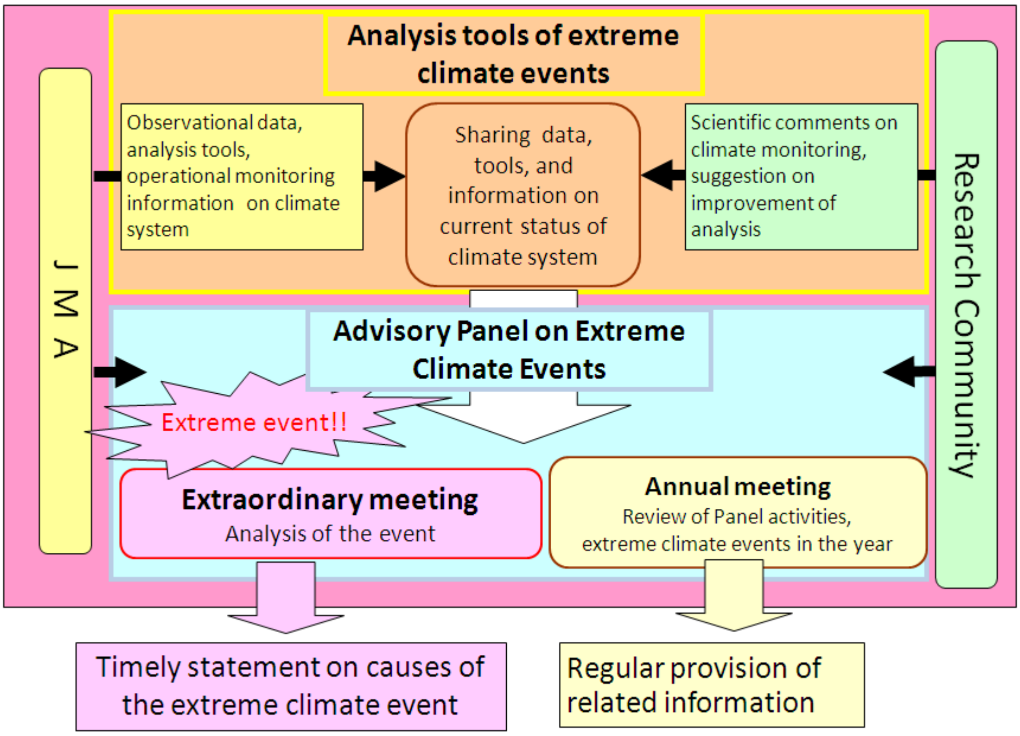

Figure 31 Framework between JMA and climate research community related to the Advisory Panel on Extreme Climate Events

Participation of TCC Experts in RCOFs and Expert Visits to NMHSs in Southeast Asia

WMO Regional Climate Outlook Forums (RCOFs) bring together national, regional and international climate experts on an operational basis to produce regional climate outlooks based on input from participating NMHSs, regional institutions, Regional Climate Centres and global producers of climate predictions. By providing a platform for countries with similar climatological characteristics to discuss related matters, these forums ensure consistency in terms of access to and interpretation of climate information.

In 2012, TCC experts participated in two RCOFs. These were the eighth session of the Forum on Regional Climate Monitoring, Assessment and Prediction for Regional Association II (FOCRAII) held in Beijing, China, from 6 to 8 April, and the third session of the South Asian Climate Outlook Forum (SASCOF-3) held in Pune, India, from 19 to 20 April. At both the events, the TCC attendees gave presentations on seasonal predictions based on JMA's numerical model and participated in discussions to produce consensus forecasts.

TCC experts also visited NMHSs in the Philippines, Viet Nam and Lao PDR in March 2012 to provide follow-up for the TCC Training Seminar on one-month forecast held in November 2011, including practical exercises with the Interactive Tool for Analysis of the Climate System (ITACS) and the installation of a module for site-specific probabilistic guidance for one-month forecasting. The experts also discussed and exchanged views with attendees on improving climate services and engaging in possible future cooperation.

(Ryuji Yamada, Tokyo Climate Center)

Presentation at FOCRA II, Beijing, China

Discussion at Philippine Atmospheric, Geophysical and Astronomical Services Administration (PAGASA), Philippines

Exercise at National Center for Hydro-Meteorological Forecasting (NCHMF), Viet Nam

Lecture at Department of Meteorology and Hydrology (DMH), Lao PDR

Any comments or inquiry on this newsletter and/or the TCC website would be much appreciated. Please e-mail to tcc@met.kishou.go.jp.

(Editors: Teruko Manabe, Ryuji Yamada and Kenji Yoshida)

Tokyo Climate Center (TCC), Climate Prediction Division, JMA
Address: 1-3-4 Otemachi, Chiyoda-ku, Tokyo 100-8122, Japan
TCC Website: http://ds.data.jma.go.jp/tcc/tcc/index.html